J Mater Sci (2019) 54:3878–3892

Composites

Design and efficient fabrication of micro-sized clusters of hydroxyapatite nanorods for dental resin composites

Shu-Ning Zhao[1,3], Dan-Lei Yang[1,3], Dan Wang[1,2,3], Yuan Pu[1,3,*], Yuan Le[1,3], Jie-Xin Wang[1,2,3,*], and Jian-Feng Chen[1,2,3]

[1] *State Key Laboratory of Organic-Inorganic Composites, Beijing University of Chemical Technology, Beijing 100029, People's Republic of China*

[2] *Beijing Advanced Innovation Center for Soft Matter Science and Engineering, Beijing University of Chemical Technology, Beijing 100029, People's Republic of China*

[3] *Research Center of the Ministry of Education for High Gravity Engineering and Technology, Beijing University of Chemical Technology, Beijing 100029, People's Republic of China*

Received: 8 October 2018
Accepted: 7 November 2018
Published online: 26 November 2018

ABSTRACT

Dental resin-based composites have been used for more than 50 years. The size and the structure of inorganic filler have a great effect on the mechanical properties of the composite resin. In this study, novel micro-sized clusters of hydroxyapatite nanorods (MCHN) were designed and conveniently fabricated by spray drying combined with heat treatment. The effects of the aspect ratio of primary hydroxyapatite nanorods (HN), suspension concentration for spray drying and heat treatment temperature were explored. The results indicated that HN with a lower aspect ratio of 2 (HN-2) and a heat treatment temperature of 500 °C were beneficial to the construction of high-performance MCHN (MCHN-2). As compared to HN-2, MCHN-2 had a further increased filling amount by 10%. More importantly, the flexural strength, flexural modulus and compressive strength of the composite resin were greatly improved by 36.3%, 11.4% and 56.6%, respectively. Therefore, it could be envisioned that MCHN could have a great potential in dental restorative application.

Introduction

A huge diversity of biomaterials have attracted great attentions due to their unique functionalities [1–3]. As an important family of biomaterials, dental resin composites have gradually replaced amalgams and are considered to be versatile and reliable materials for curing various types of dental caries because of advantageous esthetics, acceptable biocompatibility and convenient clinical manipulation [4–7]. They are mainly comprised of resin matrix (including initiator, co-initiator and inhibitors) and surface-modified inorganic fillers [8–11]. Presently, the most significant changes in dental resin composites are in the type and the structure of inorganic fillers. The effects of the size and the shape of different fillers have been

Address correspondence to E-mail: puyuan@mail.buct.edu.cn; wangjx@mail.buct.edu.cn

https://doi.org/10.1007/s10853-018-3125-3

extensively investigated [11–16]. In particular, the filler size has always been a point of concern. Larger particles (micro-particles) can allow higher filling amount and then produce superior mechanical properties, whereas difficult to polish and impossible to retain surface smoothness. Smaller particles (nanoparticles) can be more effectively polished and exhibit higher wear resistance [17–19]. However, nanoparticles have a large surface area and tend to severe agglomeration owing to the nanosize effect, thereby generating a stronger interaction between filler and matrix [20]. This will result in less filler loading, a significant increase in viscosity and the corresponding reduced mechanical properties [21]. Although the use of hybrid fillers can bridge this gap, an alternate strategy still needs to be developed to get the best of both worlds. A kind of novel filler called as "nanocluster" was thus designed, which was defined as a secondary structure or aggregation with size in the sub-micrometer or micrometer range and composed of primary nanoparticles [6, 22, 23]. Presently, sintering process and coupling reaction have been used to fabricate high-performance zirconia/silica nanoclusters or silica nanoclusters for dental resin materials [24, 25]. However, the former method needs a high sintering temperature of 1300 °C, while the latter has a relatively complicated synthetic procedure, including a first surface functionalization of SiO_2 nanoparticles and a subsequent coupling reaction [26, 27]. Furthermore, the nanoclusters formed with both routes have irregular shape and serious agglomeration. Therefore, it is very necessary to develop an efficient way for the convenient construction of regular nanoclusters with good dispersity.

The commonly used inorganic filler types have silica (SiO_2), alkaline glasses, hydroxyapatite (HA, $Ca_{10}(PO_4)_6(OH)_2$), metal oxides [such as Al_2O_3, TiO_2, ZnO and ZrO_2] and other compounds [28–32]. As the main component of dental hard tissues, HA has attracted broad attentions because of its high biocompatibility and bioactivity [33–35]. Presently, various shapes of HA such as spheroidal, rod-like, whisker and fibrous particles have been used to prepare biomimetic dental resin composites [36–38]. The related studies indicated that high-aspect-ratio HA filler-reinforced resin composites displayed better mechanical properties [39, 40]. To improve the filling properties of spheroidal and low-aspect-ratio HA nanoparticles, the concept of "nanocluster" can also be introduced into HA system. Up to now, there are no related reports on the preparation of HA nanoclusters for dental resin composites.

Spray drying is an efficient drying method, which is initiated by atomizing suspension or liquid into very tiny droplets of the order of several to hundreds of micrometers, followed by a drying process, thereby producing solid particles [41–43]. Owing to its simple and rapid processing, spray drying has been widely used in the pharmaceutical industry, food (e.g., powdered milk and animal feeds) and material processing [44]. However, no efforts were attempted to apply spray drying technology to fabricate nanocluster fillers for dental restorative composite resin. In this study, a novel route was presented to efficiently fabricate micro-sized clusters of hydroxyapatite nanorods (MCHN) by spray drying combined with heat treatment. The proper heat treatment can greatly consolidate the structure of MCHN to prevent the destruction of MCHN. The effects of the aspect ratio of primary hydroxyapatite nanorods (HN), suspension concentration for spray drying and heat treatment temperature were explored. The relationships between various factors and the mechanical properties of the resin composites were also investigated.

Materials and methods

Materials

Analytical reagent-grade ammonium hydrogen phosphate ($(NH_4)_2HPO_4$), urea ($CO(NH_2)_2$), ammonium water ($NH_3{\cdot}H_2O$), calcium nitrate tetrahydrate ($Ca(NO_3)_2{\cdot}4H_2O$), propylamine (C_3H_9N), cyclohexane (C_6H_{12}) and ethanol (C_2H_5OH) were bought from Sinopharm Chemical Reagent Beijing Co. Ltd. Bisphenol A glycerolate dimethacrylate (Bis-GMA), triethylene glycol dimethacrylate (TEGDMA), camphorquinone (CQ), 3-methacryloyl trimethoxypropylsilane (γ-MPS) and ethyl-4-dimethylaminobenzoate (4-EDMAB) were obtained from Shanghai Aladdin Bio-Chem Technology Co., Ltd. Deionized water was obtained from a Hitech-K flow water purification system (Shanghai Hogan Scientific Instrument Co. Ltd., China) and used throughout the study. Four kinds of commercially available dental resin composites were purchased from Shenyang Banner Medical Devices Co., Ltd (China) for comparative

studies, including Filtek™ Z250 with zirconia/silica nanoclusters as fillers (3M ESPE, USA), Filtek™ P60 with silica and zirconia as fillers (3M ESPE, USA), Neofil™ (Kerr, Germany) and Charisma (Heraeus, Germany) with silicate and silica as fillers. Silica nanoparticles with a size of 80 nm were prepared by Stöber method and used as a control for in vitro bioactivity testing.

Preparation of micro-sized clusters of hydroxyapatite nanorods

Primary hydroxyapatite nanorods (HN) with three aspect ratios of 2, 15 and 38 were prepared with different molar ratios (4:0, 2:2 and 0:4) of $NH_3{\cdot}H_2O$ and CO $(NH_2)_2$ as aspect ratio modifier by a high-gravity reactive precipitation in a rotating packed bed (RPB) combined with hydrothermal treatment. The corresponding HN were denoted as HN-2, HN-15 and HN-38, respectively. More preparation details can be seen in our previous paper [45]. In a typical preparation process of micro-sized clusters of hydroxyapatite nanorods (MCHN), the filter cake of HN after washing was used owing to better particle dispersion. After hydroxyapatite content in the filter cake was determined by analysis, the filter cake was directly added to the corresponding amount of deionized water to form the suspension of HN with a solid content of 2%. Subsequently, the above suspension under the stirring was pumped into the spray drier (B-290, BUCHI Labortechnik AG, Switzerland) with a flow rate of 7.6 mL/min. The temperature at the nozzle was set to 120 °C. The compressed air pressure during spray drying was 0.4 MPa. After the spray drying, the powder collected from the outlet was further heat treated at 500 °C for 3 h. The final products were denoted as MCHN-2, MCHN-15 and MCHN-38, respectively. The schematic representation of MCHN formation is shown in Scheme 1.

Modification of MCHN

The surface of MCHN was modified following the method as reported [40]. 10 g of MCHN, 1 g of γ-MPS and 0.4 g of propylamine were, respectively, added to 200 mL of cyclohexane in 1-L three-necked flask at a room temperature. After stirring for 30 min, the suspension was heated at 65 °C for 90 min. Afterward, the above mixture was firstly evaporated on a rotary evaporator at 45 °C to remove the volatile substances and then heated at 90 °C for 1 h. Finally, the product was dried in an oven under vacuum at 90 °C for 20 h.

Preparation of dental resin composites

The modified MCHN with different filler mass fractions (20 wt%, 40 wt%, 50 wt% and 60 wt%) were manually mixed by hand spatulation with a resin matrix containing 49.5 wt% Bis-GMA, 49.5 wt% diluent comonomer TEGDMA and initiators (CQ/4-EDMAB, 0.2/0.8, wt%); after the powder was thoroughly wetted with the resin matrix, the composite pastes were completely mixed into a three-roller mixer (TR50M, Trilos Precision Equipment Co., Ltd., China) with a speed of 30 rpm for thorough mixing. Afterward, the obtained composite pastes were carefully added to the rectangular (25 mm × 2 mm × 2 mm) and circle-shaped (Φ 4 mm × 6 mm) silicone molds for different mechanical performance tests covered by glass slides to prevent air-inhibited layers. The samples were photo-polymerized with a LED light curing (Blue light, 470 nm, SLC-VIII B Hangzhou Sifang Medical Apparatus Co., Ltd., China) for 60 s on each side and then stored in a dark environment at a room temperature for 3 days. Finally, all the specimens were polished using a sand paper with a grit number of 600 #.

Characterization

The surface morphologies of MCHN and fractured composites were observed with a scanning electron microscope (SEM) (JSM-6701F, JEOL, Japan). The particle size of MCHA-2 was obtained based on the measurement of over 200 particles of SEM images with image analysis and processing software (Image-Pro Plus 6.5, Media Cybernetics Inc., USA). The size and the morphology of HN were characterized with a transmission electron microscopy (TEM) (JEOL-7800, JEOL, Japan) at an accelerating voltage of 120 kV. The crystalline form of MCHN was detected by powder X-ray diffraction (XRD-6000, Shimadzu, Japan) equipped with Cu Kα radiation (λ = 0.1541 nm) at 40 kV and range from 20° to 60° at a scanning rate of 5°/min. Fourier transform infrared (FTIR) data were recorded in the range of 3500–400 cm^{-1} with a Nicolet 6700 spectrometer (Nicolet Instrument Co., USA). Thermogravimetric (TG) analysis was

Scheme 1 Schematic diagram of the preparation of MCHN.

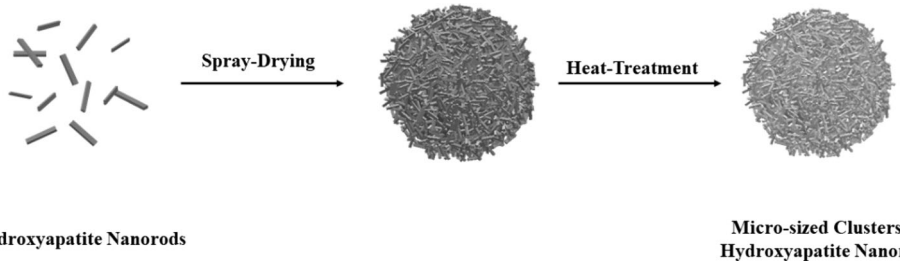

performed on a thermogravimetric analyzer (STA-449C, NETZSCH, Germany) from 40 to 800 °C with a heating rate of 10 °C/min in the N_2 atmosphere. The Brunauer–Emmett–Teller (BET) specific surface area was measured by nitrogen isothermal adsorption equipment (QUADRASORB SI, Quadrasorb SI, America).

The related mechanical properties of dental resin composites containing HN or MCHN were detected by a universal mechanical testing machine [CMT6503, MTS Industrial Systems (China) Co., Ltd.]. Flexural properties were measured following International Standard Organization (ISO) Specification No. 4049. Six specimens with a size of 25 mm × 2 mm × 2 mm were prepared from each material. The samples were bent in a universal testing machine with a distance between the two supports of 20 mm. All bend tests were performed with a constant crosshead speed of 0.75 mm/min until the fracture occurred. Six specimens (Φ 4 mm × 6 mm) were tested in compression mode using the universal testing machine to measure their compression strength. The samples were loaded to broken in compression at a crosshead speed of 0.75 mm/min.

In vitro bioactivity was investigated by evaluating apatite forming ability of the resin composite in simulated body fluid (SBF). Typical testing process is as follows. Disk specimens with a diameter of 10 mm and a thickness of 1 mm were soaked in 20 mL SBF at 37 °C for 1 d and 30 d, respectively. SBF was renewed once a week. After the soaking finished, the specimens were taken out and washed with deionized water several times, followed by the drying in an oven at 60 °C for 24 h. Finally, the surface morphology and the chemical composition of the composite resins after the soaking in SBF for 0 d, 1 d and 30 d were analyzed by SEM equipped with an energy-dispersive X-ray spectroscopy (EDS, Quantax, Bruker, Germany).

Results and discussion

Figure 1 shows SEM images of MCHN-2 obtained by spray drying the suspension with different solid contents. When the solid content of the suspension was 1% or 2%, almost all the HN-2 were constructed to form micro-sized clusters with a spherical shape, a size of 1–4 μm and good dispersion (Fig. 1a, b). A higher-magnification SEM image (Fig. 1d) clearly revealed that lots of HN-2 were tightly flocked together to form MCHN-2, and the morphology and size of the primary nanorods did not change appreciably. However, when the solid content was further increased to 3%, many separate HN-2 were observed, and not constructed into MCHN-2. Furthermore, in this case, the suspension was viscous, which easily blocked the nozzle. So the solid content of 2% was selected in the following study.

Figure 2 displays representative TEM images of primary HN-2, HN-15, HN-38 and SEM images of the corresponding as-prepared MCHN-2, MCHN-15 and MCHN-38. Owing to the lower aspect ratio of HN-2, the formed MCHN-2 appeared a regular spherical structure with a tight arrangement of nanorods (Fig. 2b). With the increase in aspect ratio of primary nanorods from 2 to 15, although MCHN were still well constructed, the regular degree of the corresponding micro-sized spherical clusters became worse. More interspace and some cavities were also found on the surface of MCHN-15 (Fig. 2d). When HN-38 with larger aspect ratio were used, only part of nanorods were constructed into micro-sized clusters. The morphology turned more irregular. Moreover, there were large amount of thicker and longer nanorods (Fig. 2f), which were hard to form MCHN. This is because the generated droplets from the nozzle have a size of about several microns, which is larger than the size of these uneasily broken nanorods. Therefore, spherical or lower-aspect-ratio particles are more suitable for spray drying to build

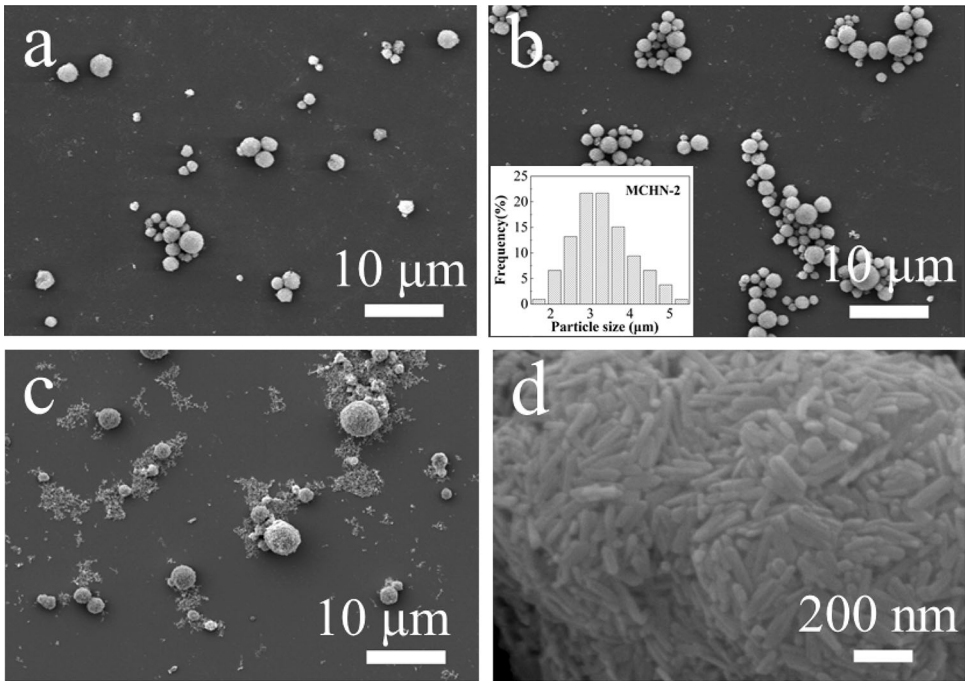

Figure 1 SEM images of MCHN-2 prepared using the suspensions with different solid contents (**a** 1%; **b** 2%; **c** 3%; **d** 2%, higher magnification of MCHN-2). The inset is particle size distribution of MCHN-2.

micro-sized clusters with regular shape and good dispersion.

To make the structure of MCHN-2 stronger for better application, the heat treatment was used. However, much higher heat treatment temperature is also improper owing to the possible structure damage. Figure 3 presents SEM images of MCHN-2 obtained at different heat treatment temperatures. It could be seen there were no obvious changes in the morphology and structure of MCHN-2 after they were calcined at 400 °C, 500 °C and 600 °C for 3 h. The insets further showed that the nanorods on the surfaces of MCHN-2 almost kept unchanged. However, when heat treatment temperature was increased to 700 °C, hydroxyapatite nanorods melted into spheroid shapes (Fig. 3e).

Figure 4 presents XRD patterns of MCHN-2 prepared at different heat treatment temperatures. All the samples (curves a-e) had six typical diffraction peaks at 2θ = 25.9°, 31.8°, 32.8°, 46.8°, 49.5° and 53.1°, which well confirmed to the standard card (JCPDS NO. 74-0565). After heat treatment, the characteristic diffraction peaks became stronger, suggesting the improved crystallinity degree of MCHN-2 [46].

Figure 5 exhibits FTIR spectra (A) and TG curves (B) of different MCHN samples. As shown in Fig. 5A, the characteristic peaks bands at 1089, 1035 and 560 cm^{-1} could be ascribed to phosphate stretching, indicating that these samples were crystalline hydroxyapatite. As compared to curve a (unmodified sample), curves b, c, d and e (modified samples) had the characteristic peaks of carbonyl (C=O) at 1722 cm^{-1}, deriving from the carbonyl bond in the molecular structure of γ-MPS as modifier. Furthermore, this characteristic peak obviously became weakened from curve b to e, especially in curves d and e. The possibly reason is because hydroxyl groups on the surface of MCHN decreased after heat treatment, thereby resulting in the reduced grafting locations of γ-MPS. And the specific surface area of MCHN decreased (60.67 m^2/g for MCHN-2, 44.61 m^2/g for MCHN-15 and 28.38 m^2/g for MCHN-38) with the increased aspect ratio of primary HN, leading to the decreased modification amount on the surfaces of MCHN-15 and MCHN-38. The accurate amounts of γ-MPS chemically attached to the surface of MCHN were further determined by TG analysis (Fig. 5B). The small weight loss below 250 °C could be ascribed to the decomposition of small molecules (such as γ-MPS and water molecules) physically adsorbed on the surface of MCHN [39, 40, 47]. Owing to the morphological change of HCHN after heat treatment at 700 °C, the weight loss between 250 and 700 °C was adopted to analyze and calculate the grafting ratio of γ-MPS onto the surfaces of MCHN. In curve a (unmodified sample), the mass loss was determined to be about 1.58%. By comparison with curve a, curves b, c, d and e (modified

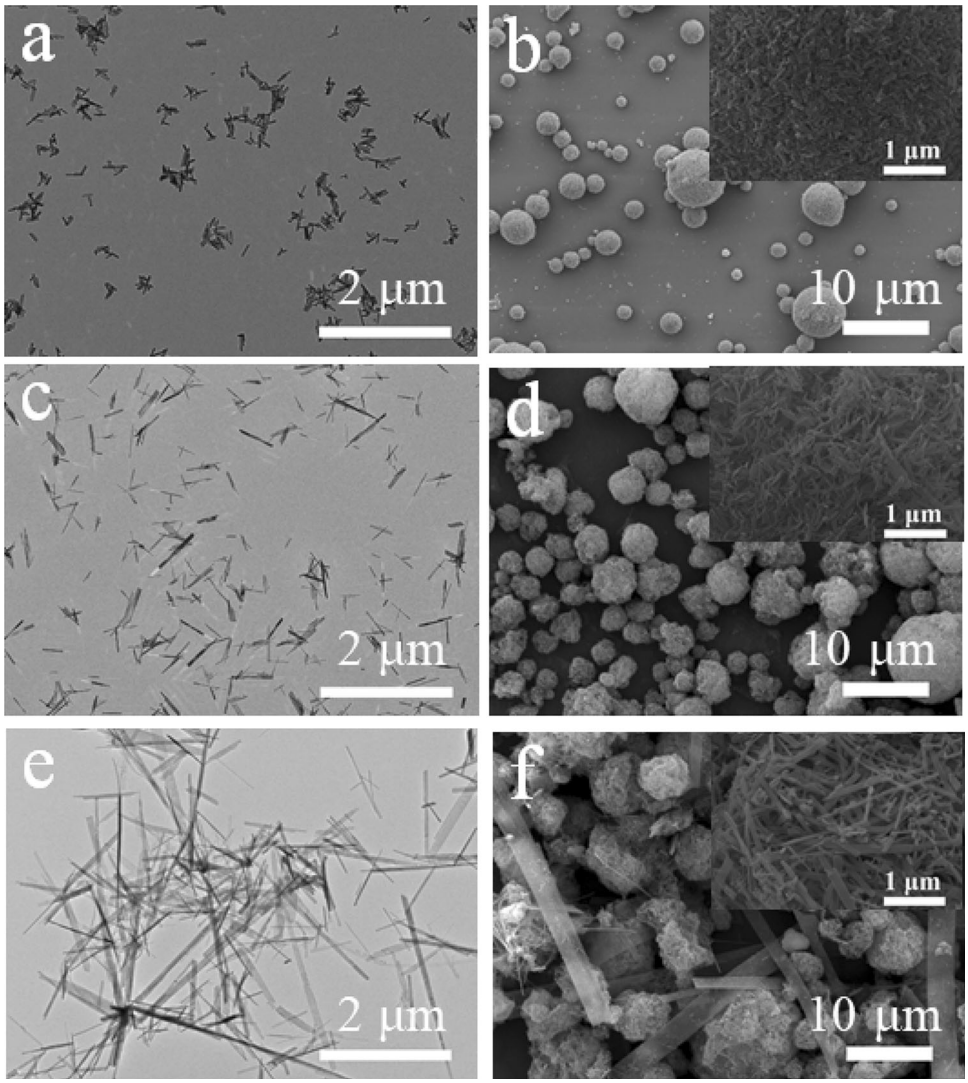

Figure 2 TEM images of primary HN with different aspect ratios (**a** HA-2; **c** HA-15; **e** HA-38) and SEM images of the as-prepared MCHN (**b** MCHN-2; **d** MCHN-15; **f** MCHN-38).

samples) had an increase in the mass loss mainly owing to the decomposition of γ-MPS grafted onto the surface of MCHN. Table 1 gives the comparison of the grafting ratio of γ-MPS on the surfaces of different MCHN samples. Without heat treatment, MCHN-2 had a highest grafting ratio of 6.57%. After the calcination treatment, the grafting ratio of MCHN-2 obviously decreased to 4.25%. And MHCN-38 had the lowest grafting ratio owing to higher aspect ratio, lower surface area and only partially construction of MHCN.

Excellent mechanical properties of the resin composites are very important in the clinic applications of dental restoration. Figure 6 shows flexural strength, flexural modulus and compressive strength of the resin composites filled with 50 wt% modified MCHN-2 obtained at different heat treatment temperatures. Compared to the unheated MCHN-2 (0 °C), the calcined MCHN-2 endowed the composites the obviously improved mechanical properties. With the increase in heat treatment temperature from 400 to 700 °C, the related mechanical properties firstly increased and then decreased, reaching the highest value at 500 °C possibly owing to the greatly consolidated micro-/nanostructure of clusters. The flexural strength, flexural modulus and compressive strength of the composite resin were thus improved by 32.6%, 19.5% and 26.2%, respectively. However, higher treatment temperatures of 600 °C and 700 °C would destroy the hydroxyl groups on the surface of MCHN, thereby resulting in lower grafting ratio, the corresponding poor compatibility and interfacial binding between MCHN-2 and the resin.

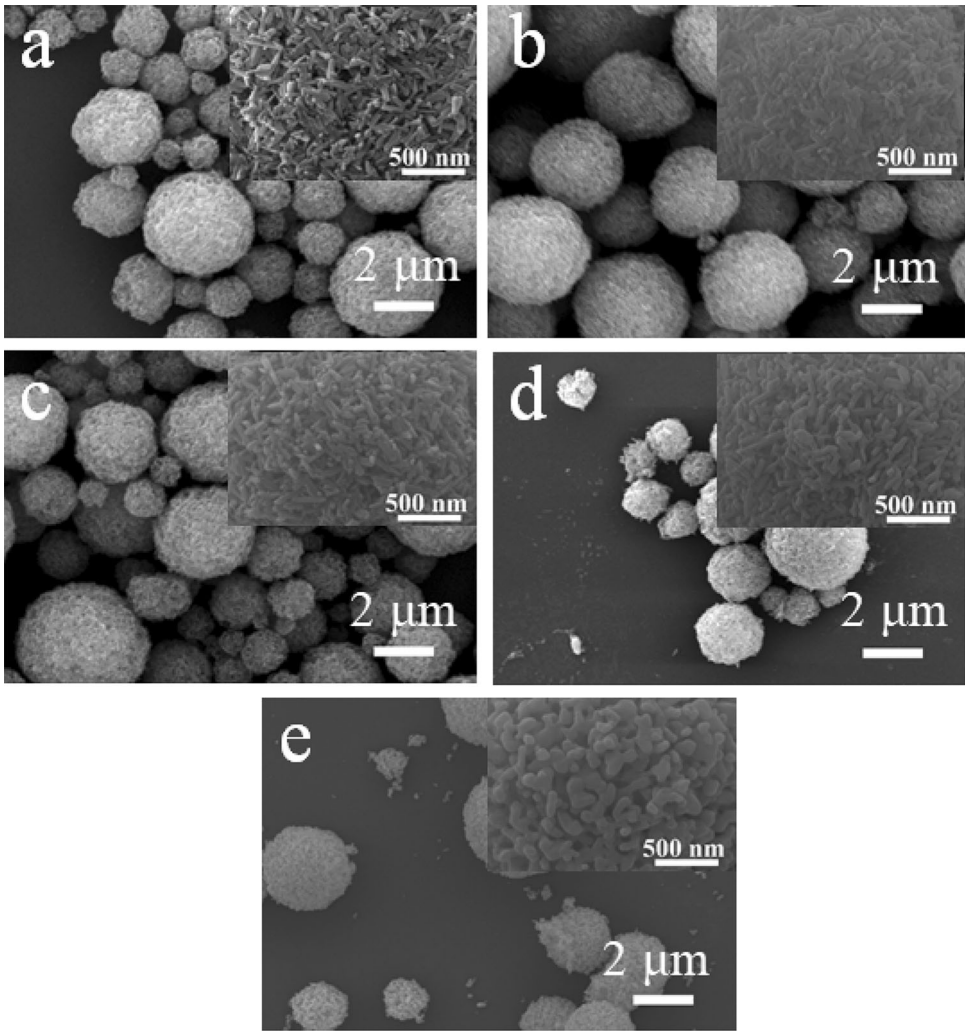

Figure 3 SEM images of MCHN-2 prepared at different heat treatment temperatures (**a** without heat treatment: **b** 400 °C; **c** 500 °C; **d** 600 °C; **e** 700 °C).

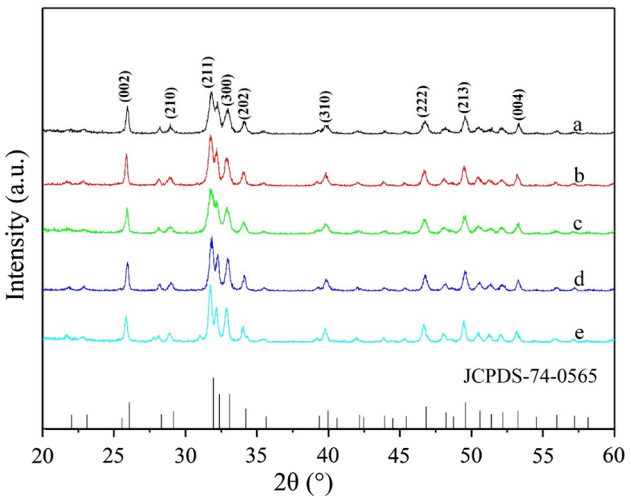

Figure 4 XRD patterns of MCHN-2 prepared at different heat treatment temperatures (a: without heat treatment: b: 400 °C; c: 500 °C; d: 600 °C; e: 700 °C).

Figure 7 shows the mechanical properties of the resin composites filled with 50 wt% MCHN-2, MCHN-15 and MCHN-38. As the aspect ratio of the primary HN increased, the constructed second microstructures had the obviously decreased filling properties. As a result, MCHN-2 exhibited the best mechanical properties. This was because MCHN-2 had a more regular spherical morphology and more compact cluster structure, as shown in Fig. 2. Such a compact aggregation of nanoparticles was more beneficial to creating an interconnected network where the interstices were infiltrated with γ-MPS, thereby forming an interpenetrating phase composite structure, resulting in the improved damage resistance and subsequent reinforcement with the resin matrix [48].

Figure 8 compares the mechanical properties of the composite resins filled with HN-2 and MCHN-2. It was obviously seen that the composite resin filled

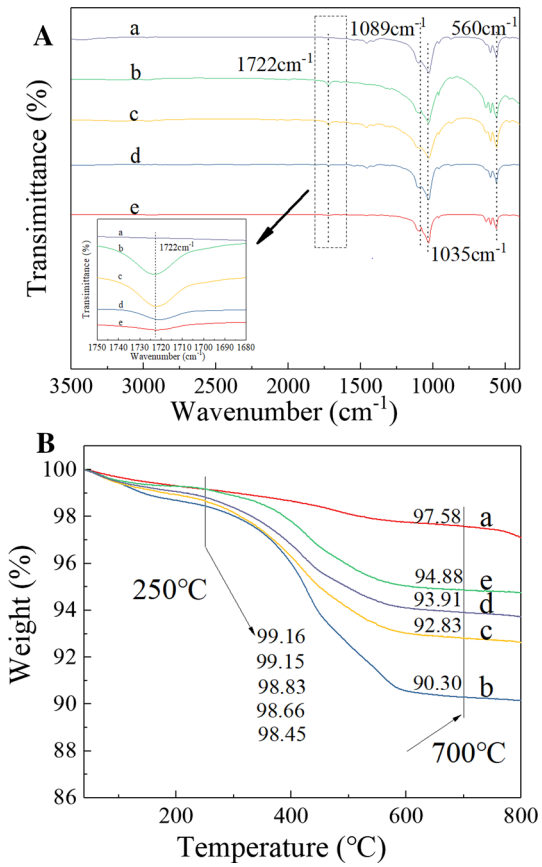

Figure 5 FTIR spectra (**A**) and TG curves (**B**) of different samples (a: unmodified MCHN-2; b: modified MCHN-2 without heat treatment; c: modified MCHN-2 treated at 500 °C; d: modified MCHN-15 treated at 500 °C; e: modified MCHN-38 treated at 500 °C).

Table 1 Grafting ratios of γ-MPS onto the surfaces of different MCHN samples

MCHN sample	Grafting ratio (wt%)
MCHN-2 without heat treatment	6.57
MCHN-2 treated at 500 °C	4.25
MCHN-15 treated at 500 °C	3.34
MCHN-38 treated at 500 °C	2.69

with MCHN-2 had much better mechanical properties than the counterpart because of the enhancement of the interfacial combination with the resin from unique micro-/nanostructure of the filler, especially in compressive strength and flexural strength [9]. When the filler content of MCHN-2 was 50 wt%, flexural strength, flexural modulus and compressive strength were (119.1 ± 5.2) MPa, (5760.6 ± 264.3) MPa and (414.9 ± 12.8) MPa, having improvements of 36.3%, 11.4% and 56.6%, respectively. Furthermore, the corresponding loading amount was also increased by 10 wt%. HN-2 could only reach the maximum filling amount of 50%. A continuous resin paste was very hard to be formed when passing through the three-roller mixer, making it difficult to carry out the next step. For MCHN-2 filler system, the flexural strength and the compressive strength of the composites had a firstly rapid increase and the following decrease with the increased filling amount from 0 to 60 wt%, respectively, reaching the maximum values of 119.1 MPa and 414.9 MPa at 50 wt%. This is because excessive filling amount will hinder and limit the movement of the particles, which affects the light curing process and ultimately results in a decrease in mechanical properties [49]. The similar rule could also be found in the HN-2 filler system. In addition, the flexural modulus continuously increased from 1375.4 to 6283.5 MPa with increasing filling amount 0 to 60 wt%.

Figure 9 displays representative SEM images of cross-sectional fracture surfaces of unfilled resin and resin composites prepared with 50 wt% MCHN-2 after three-point bending test. As shown in Fig. 9a, the unfilled resin had a flat fracture surface, indicating little resistance of the sample to the applied force. And the cross section had layered and brittle fracture. In comparison, the resin filled with MCHN-2 appeared the rough fracture surfaces with numerous curved and stretched steps (Fig. 9b, c), implying that MCHN-2 could deflect the cracks, and the composites had higher fracture energy than the unfilled resin [9]. Furthermore, MCHN-2 were nearly observed without heat treatment (Fig. 9b), because of the easy destruction of the weak structure of MCHN-2 when passing through a three-roller mixer. Contrastively, MCHN-2 with a heat treatment of 500 °C were uniformly and closely distributed in the resin (Fig. 9c), completely proving that the structure of MCHN-2 had been strengthened by heat treatment. A higher-magnification SEM image of MCHN-2 (Fig. 9d) revealed that the mutual permeating structure was formed in the middle of fillers and the dental matrix [48]. This may deflect crack or dissipate the energy of the propagating crack tip effectively.

Table 2 gives the comparison of mechanical properties of reported dental resin composites using different shaped hydroxyapatite as fillers. Clearly, the mechanical properties of our product were similar to or much higher than those of other reported

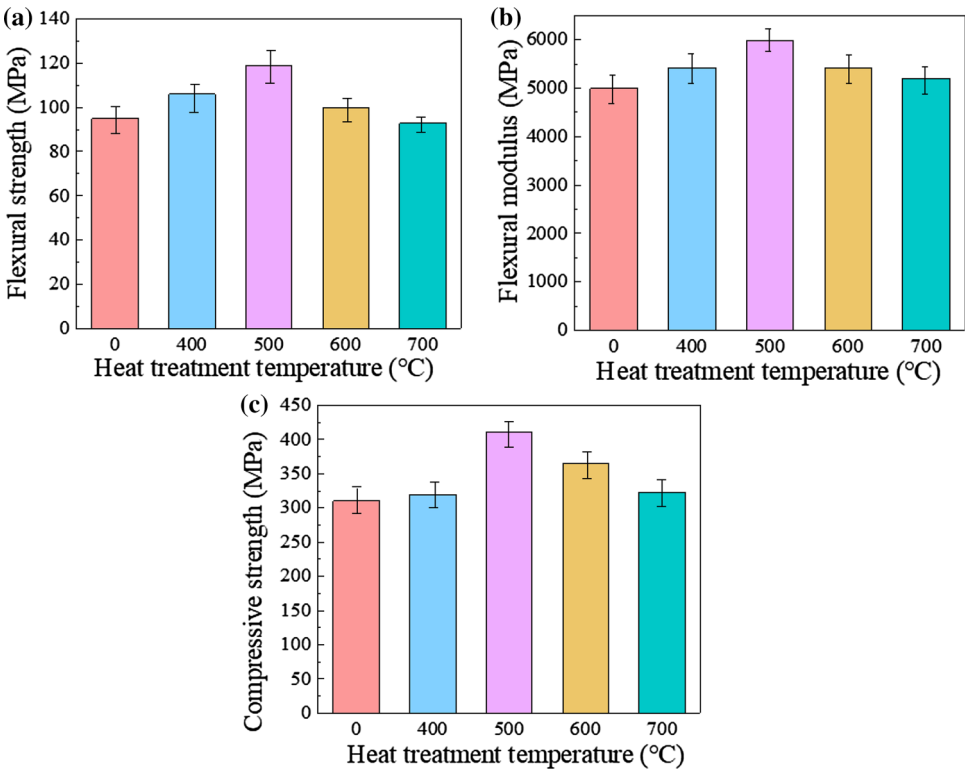

Figure 6 Flexural strength (**a**), flexural modulus (**b**) and compressive strength (**c**) of the resin composites filled with MCHA-2 obtained at different heat treatment temperatures.

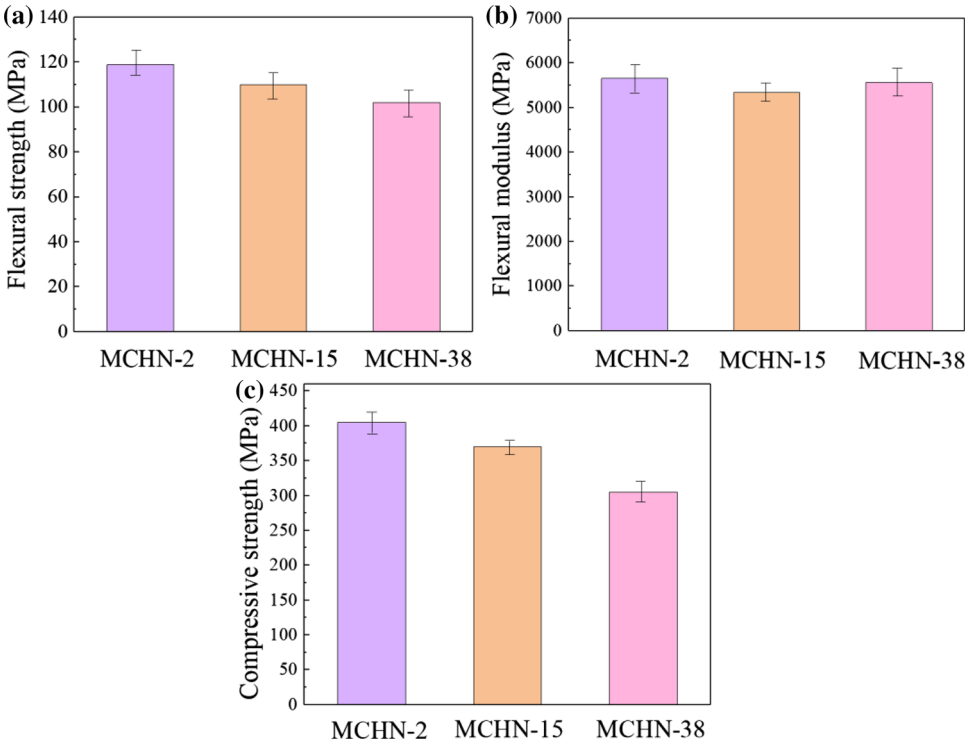

Figure 7 Flexural strength (**a**), flexural modulus (**b**) and compressive strength (**c**) of the resin composites filled with MCHN-2, MCHN-15 and MCHN-38.

hydroxyapatite-filled resin composites. In particular, the highest mechanical properties were achieved at a high filler loading content of 50 wt%, which was important for practical application. This is because resin composites have cytotoxic effects that can occur because of the release of free monomers during the

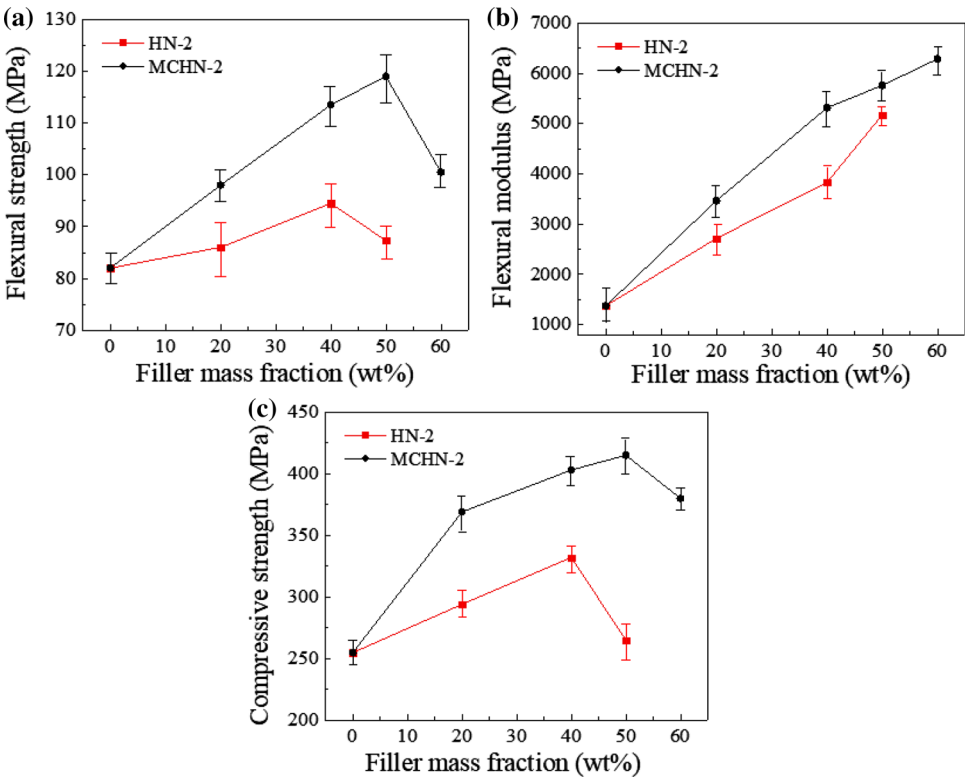

Figure 8 Flexural strength (**a**), flexural modulus (**b**) and compressive strength (**c**) of the resin composites filled with HN-2 and MCHN-2.

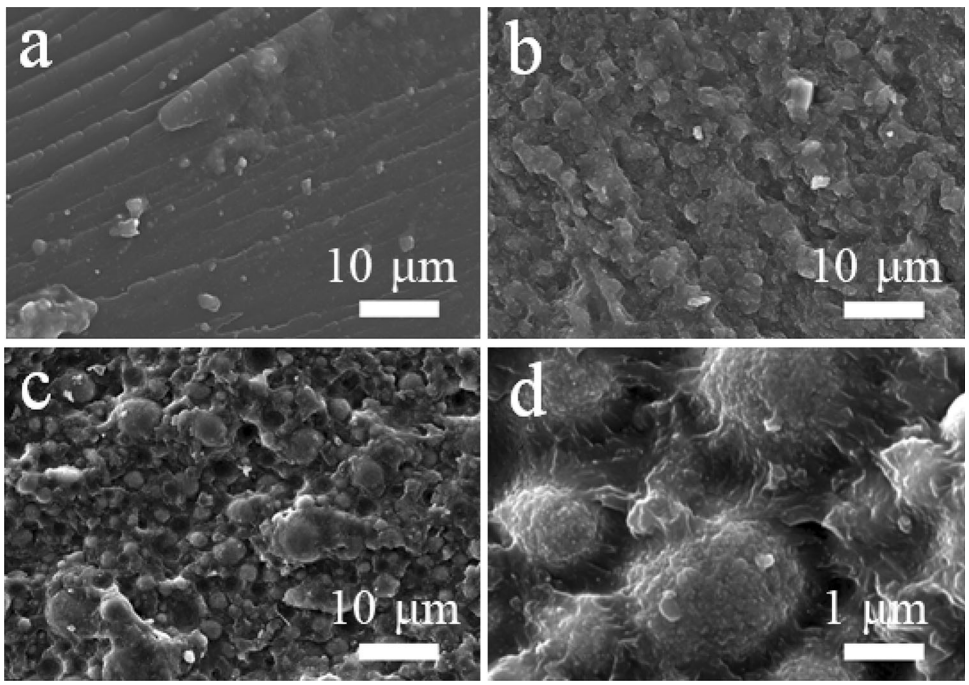

Figure 9 SEM images of fracture surfaces of unfilled resin (**a**), resins filled with MCHN-2 without heat treatment (**b**), MCHN-2 treated at 500 °C (**c**) and the corresponding higher magnification (**d**).

monomer–polymer conversion [51]. Therefore, once the monomers are selected, decreasing the resin ratio by increasing the loading amount of inorganic filler may be the most effective way to avoid toxicity of oral cells in contact with restorations [15]. And an increase in the mass fraction of the filler can reduce polymerization shrinkage, thermal expansion and moisture absorption [52, 53]. Furthermore, we also purchased four kinds of representative commercially available composite resins with zirconia/silica

Table 2 Mechanical properties of reported typical dental resin composites using different shaped hydroxyapatite as fillers

Reference	Morphology	Filling amount (wt%)	Flexural strength (MPa)	Compressive strength (MPa)
Our work	Cluster	50	120	410
[50]	Spheroidal	62.5	95	–
[40]	Whisker	48	105	223
[37]	Whisker	10	124	370
[10]	Urchin-like	20	119	388

nanoclusters or silica/silicate glass particles as fillers and tested them on the same instrument for a better comparison. The corresponding flexural strength, flexural modulus and compressive strength are shown in Fig. 10. Although it had the lower flexural strength than the well-known Filtek^{TM} Z250 filled with zirconia/silica nanoclusters from 3M ESPE, our product was still superior to other commercial products from different companies including another 3M product. More importantly, according to International Standard Organization (ISO) Specification No. 4049, the flexural strength of dental resin composite is required to reach > 80 MPa. The flexural strength of our product is 50% higher than the requirement. For flexural modulus, our product was much lower than both 3M products, while slightly higher than other both commercial products from Germany. Surprisingly, the compressive strength of our product was higher or much higher than four commercial counterparts. In addition, as compared to silica fillers, it is commonly accepted that as the main component of dental hard tissues, hydroxyapatite possesses high biocompatibility and bioactivity such as remineralization [33–35].

In vitro bioactivity is defined as the ability of a material to form apatite layer on its surface when soaked in SBF [54]. To better understand the difference of the bioactivity of hydroxyapatite and silica, the resin composites filling MCHN-2 and silica nanoparticles with a size of 80 nm were evaluated. Figure 11 presents SEM images of the surfaces of the resin composites filled with SiO_2 nanoparticles and MCHN-2 after the soaking in SBF for 0 d, 1 d and 30 d, and the corresponding EDS spectra after the soaking in SBF for 30 d. It could be observed that there was an obvious mineral precipitation on the surface of the resin composite containing MCHN-2 filler after 1 d (Fig. 11e). After the soaking for 30 d, the surface was covered with a denser and continuous layer (Fig. 11f). In comparison, the surface of the resin composite with SiO_2 filler was only covered with discrete particles even after 30 d (Fig. 11c), clearly demonstrating that it had a much weaker remineralization effect. Furthermore, EDS analysis indicated that the main elements of the formed layer on the surface of the resin composite containing MCHN-2 were oxygen, calcium and phosphorus after the soaking for 30 d (Fig. 11h). Carbon and a small amount of silicon may come from the resin matrix and the modifier of γ-MPS. For the surface of the resin composite containing SiO_2, a small amount of calcium and phosphorus besides the main elements of oxygen and silicon from SiO_2 was also detected (Fig. 11g), mainly owing to weak remineralization in SBF. In addition, Ca/P atomic ratios were analyzed to be about 1.50 and 1.63 for the composite systems filled with SiO_2 and MCHN-2, respectively, which were less than the stoichiometric ratio 1.67 of hydroxyapatite, indicating that the precipitated layers were calcium-deficient apatite [55]. The above results demonstrated that the resin composites filled with MCHN-2 owned a better bioactivity, and could have the potential to improve marginal adaptation of restoration and remineralization restoration to reduce the occurrence of secondary caries [33, 36, 39]. In the future, in situ studies on natural teeth will be further needed to test whether the apatite layer can be formed between resin composite and teeth, and its stability under simulated wet oral surroundings.

Conclusions

In this study, a novel route was developed to efficiently prepare micro-sized clusters of hydroxyapatite nanorods (MCHN) as designed inorganic filler for dental resin composites by the combination of spray drying and heat treatment. MCHN with a size of 1–4 μm, regular shape and good dispersion could be achieved using HN with a lower aspect ratio of 2

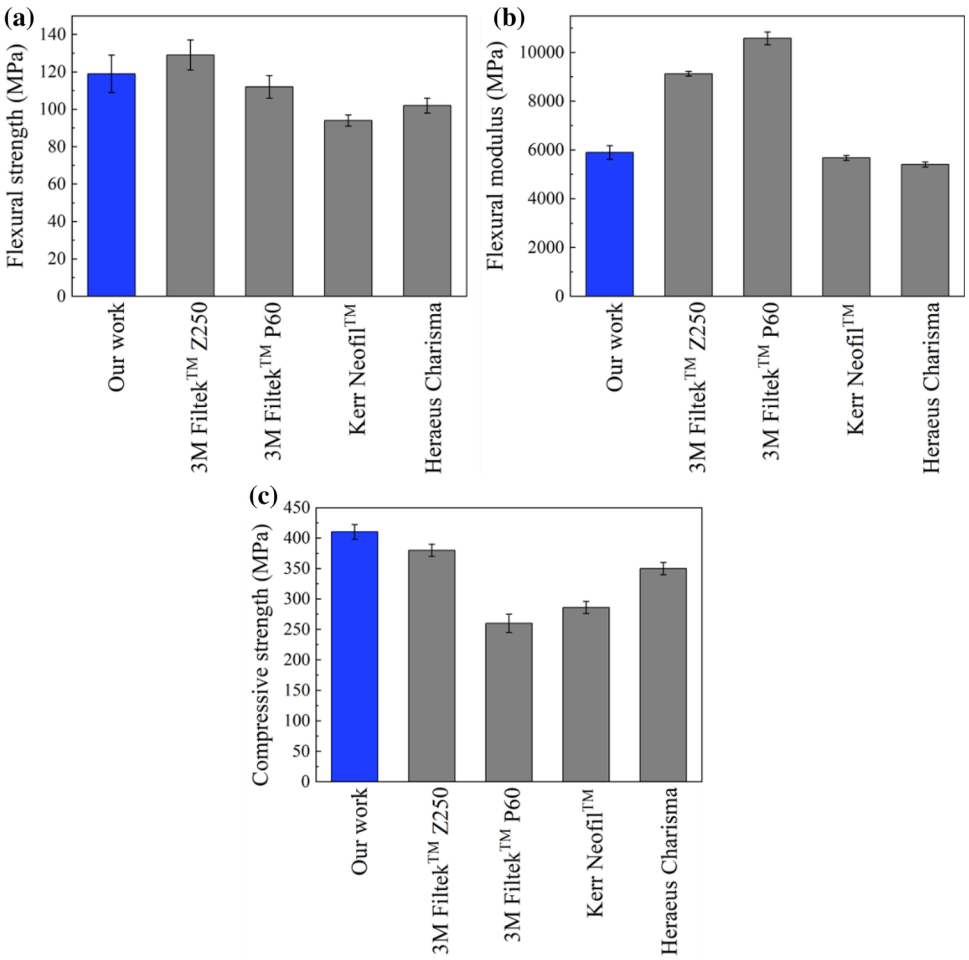

Figure 10 Flexural strength (**a**), flexural modulus (**b**) and compressive strength (**c**) of the resin composite filled with MCHN-2 and four kinds of commercially available resin composites.

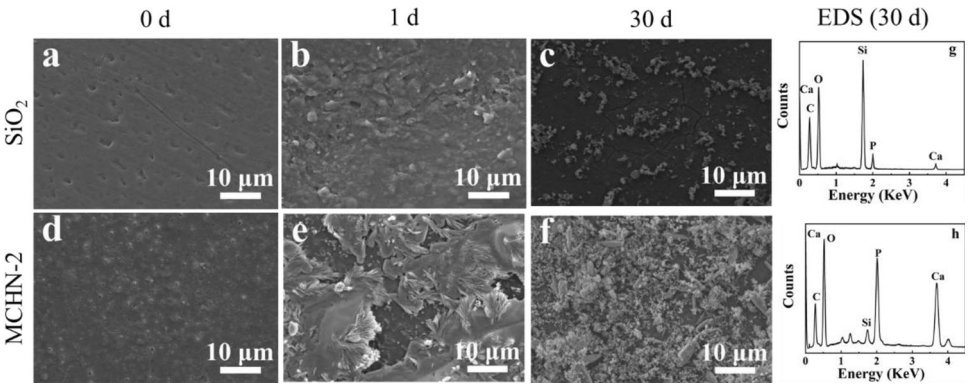

Figure 11 SEM images of the surfaces of the resin composites filled with SiO_2 nanoparticles (**a**, **b**, **c**) and MCHN-2 (**d**, **e**, **f**) after the soaking in SBF for 0 d, 1 d and 30 d, and the corresponding EDS spectra (**g** SiO_2, **h** MCHN-2) after the soaking in SBF for 30 d.

(HN-2) as primary nanoparticles and heat treatment temperature of 500 °C. The effects of the aspect ratio of primary HN, the heat treatment temperatures and the filling amount on the mechanical properties of the resin composites were further investigated. By comparison with MCHN-15 and MCHN-38, the resin filled with MCHN-2 showed the best mechanical properties. As compared to HN-2, MCHN-2 had an increased filling amount by 10%. More importantly, when the filling content of MCHN-2 was 50 wt%, the flexural strength, flexural modulus and compressive strength of the composites reached (119.1 ± 5.2) MPa, (5760.6 ± 264.3) MPa and (414.9 ± 12.8) MPa, respectively, realizing great improvements of 36.3%, 11.4% and 56.6%. It could be envisioned that this route for preparing micro-sized

clusters of nanoparticles could be expanded to the development of other types of dental inorganic fillers.

Acknowledgements

This work was financially supported by the National Key Research and Development Program of China (2016YFA0201701/2016YFA0201700), National Natural Science Foundation of China (21878015 and 21622601) and National Key Basic Research Program of China (2015CB932100).

References

[1] Qi C, Lin J, Fu LH, Huang P (2018) Calcium-based biomaterials for diagnosis, treatment, and theranostics. Chem Soc Rev 47:357–403

[2] Lv SS, Dudek DM, Cao Y, Balamurali MM, Gosline J, Li HB (2010) Designed biomaterials to mimic the mechanical properties of muscles. Nature 465:69–73

[3] Wang D, Wang ZY, Zhan QQ, Pu Y, Wang JX, Foster NR, Dai LM (2017) Facile and scalable preparation of fluorescent carbon dots for multifunctional applications. Engineering 3:402–408

[4] Duraccio D, Mussano F, Faga MG (2015) Biomaterials for dental implants: current and future trends. J Mater Sci 50:4779–4812. https://doi.org/10.1007/s10853-015-9056-3

[5] Volpe JJ (2009) Brain injury in premature infants: a complex amalgam of destructive and developmental disturbances. Lancet Neurol 8:110–124

[6] Habib E, Wang RL, Wang YZ, Zhu MF, Zhu XX (2016) Inorganic fillers for dental resin composites: present and future. ACS Biomater Sci Eng 2:1–11

[7] Miao XL, Li YG, Zhang QH, Zhu MF, Wang HZ (2012) Low shrinkage light curable dental nanocomposites using SiO_2 microspheres as fillers. Mater Sci Eng, C 32:2115–2121

[8] Habib E, Wang RL, Zhu XX (2018) Correlation of resin viscosity and monomer conversion to filler particle size in dental composites. Dent Mater 34:1501–1508

[9] Karabela MM, Sideridou ID (2011) Synthesis and study of properties of dental resin composites with different nanosilica particles size. Dent Mater 27:825–835

[10] Liu FW, Sun B, Jiang XZ, Aldeyab SS, Zhang QH, Zhu MF (2016) Mechanical properties of dental resin/composite containing urchin-like hydroxyapatite. Dent Mater 30:358–368

[11] Kaizer MR, de Oliveira-Ogliaria A, Cenci MS, Opdam NJ, Moraes RR (2014) Do nanofill or submicron composites show improved smoothness and gloss? A systematic review of in vitro studies. Dent Mater 30:e41–e78

[12] Robertson CG, Lin CJ, Rackaitis M, Roland CM (2008) Influence of particle size and polymer-filler coupling on viscoelastic glass transition of particle-reinforced polymers. Macromolecules 41:2727–2731

[13] Valente LL, Peraltaa SL, Ogliarib FA, Cavalcantec LM, Moraesa RR (2013) Comparative evaluation of dental resin composites based on micron- and submicron-sized monomodal glass filler particles. Dent Mater 29:1182–1187

[14] Ferracane JL (2016) Current trends in dental composites. Crit Rev Oral Biol Med 6:302–318

[15] Attik N, Hallay F, Bois L, Brioude A, Grosgogeat B, Colon P (2017) Mesoporous silica fillers and resin composition effect on dental composites cytocompatibility. Dent Mater 33:166–174

[16] Habib E, Wang RL, Zhu XX (2017) Monodisperse silica-filled composite restoratives mechanical and light transmission properties. Dent Mater 33:280–287

[17] Ferracane JL (2011) Resin composite-State of the art. Dent Mater 27:29–38

[18] Turssi CP, Ferracane JL, Vogel K (2005) Filler features and their effects on wear and degree of conversion of particulate dental resin composites. Biomaterials 26:4932–4937

[19] Cavalcante LM, Masouras K, Watts DC, Pimenta LA, Silikas N (2009) Effect of nanofillers' size on surface properties after toothbrush abrasion. Am J Dent 22:60–64

[20] Nagarajan VS, Jahanmir S, Thompson VP (2004) In vitro contact wear of dental composites. Dent Mater 20:63–71

[21] Lee JH, Um CM, Lee IB (2006) Rheological properties of resin composites according to variations in monomer and filler composition. Dent Mater 22:515–526

[22] Hu X, Gong J, Zhang L, Yu JC (2008) Continuous size tuning of monodisperse ZnO colloidal nanocrystal clusters by a microwave-polyol process and their application for humidity sensing. Adv Mater 20:4845–4850

[23] Wang RL, Habib E, Zhu XX (2018) Evaluation of the filler packing structures in dental resin composites: from theory to practice. Dent Mater 34:1014–1023

[24] Mitra SB, Wu D, Holmes BN (2003) An application of nanotechnology in advanced dental materials. J Am Dent Assoc 134:1382–1390

[25] Atai M, Pahlavan A, Moin N (2012) Nano-porous thermally sintered nano silica as novel fillers for dental composites. Dent Mater 28:133–145

[26] Wang RL, Bao S, Liu FW, Jiang XZ, Zhang QH, Sun B, Zhu MF (2013) Wear behavior of light-cured resin composites with bimodal silica nanostructures as fillers. Mater Sci Eng, C 33:4759–4766

[27] Wang RL, Zhang ML, Liu FW, Bao S, Wu TT, Jiang XZ, Zhang QH, Zhu MF (2015) Investigation on the physical-mechanical properties of dental resin composites reinforced with novel bimodal silica nanostructures. Mater Sci Eng, C 50:266–273

[28] Lenji RK, Nourbakhsh AA, Nourbakhsh N, Nourbakhsh M, Mackenzie KJD (2017) Phase formation, microstructure and setting time of MCM-48 mesoporous silica nanocomposites with hydroxyapatite for dental applications: effect of the Ca/P ratio. Ceram Int 43:12857–12862

[29] Saen P, Atai M, Nodehi A, Solhi L (2016) Physical characterization of unfilled and nanofilled dental resins: static versus dynamic mechanical properties. Dent Mater 32:185–197

[30] Thorat SB, Diaspro A, Salerno M (2013) Effect of alumina reinforcing fillers in BisGMA-based resin composites for dental applications. Adv Mater Lett 4:15–21

[31] Yoshida K, Tanagawa M, Atsuta M (2001) Effects of filler composition and surface treatment on the characteristics of opaque resin composites. J Biomed Mater Res 58:525–530

[32] Thorat SB, Patra N, Ruffilli R, Diaspro A, Salerno M (2012) Preparation and characterization of a BisGMA-resin dental restorative composites with glass, silica and titania fillers. Dent Mater 31:635–644

[33] Liu FW, Jiang XZ, Zhang QH, Zhu MF (2014) Strong and bioactive dental resin composite containing poly(Bis-GMA) grafted hydroxyapatite whiskers and silica nanoparticles. Compos Sci Technol 101:86–93

[34] Suchanek K, Bartkowiak A, Gdowik A, Perzanowski M, Kąc S, Szaraniec B, Suchanek M, Marszałeka M (2015) Crystalline hydroxyapatite coatings synthesized under hydrothermal conditions on modified titanium substrates. Mater Sci Eng C Mater Biol Appl 51:57–63

[35] Singh B, Tandon A, Pandey AK, Singh P (2018) Enhanced dielectric constant and structural transformation in Fe-doped hydroxyapatite synthesized by wet chemical method. J Mater Sci 53:8807–8816. https://doi.org/10.1007/s10853-018-2225-4

[36] Andrade Neto DM, Carvalho EV, Rodrigues EA, Feitosa VP, Sauro S, Mele G, Carbone L, Mazzetto SE, Rodrigues LK, Fechine PBA (2016) Novel hydroxyapatite nanorods improve anti-caries efficacy of enamel infiltrants. Dent Mater 32:784–793

[37] Liu FW, Bao S, Jin Y, Jiang XZ, Zhu MF (2014) Novel bionic dental resin composite reinforced by hydroxyapatite whisker. Mater Res Innov 18:854–858

[38] Zhang H, Darvell BW (2012) Mechanical properties of hydroxyapatite whisker-reinforced bis-GMA-based resin composites. Dent Mater 28:824–830

[39] Chen L, Yu QS, Wang Y, Li H (2011) BisGMA/TEGDMA dental composite containing high aspect-ratio hydroxyapatite nanofibers. Dent Mater 27:1187–1195

[40] Liu FW, Wang RL, Cheng YH, Jiang XZ, Zhang QH, Zhu MF (2013) Polymer grafted hydroxyapatite whisker as a filler for dental composite resin with enhanced physical and mechanical properties. Mater Sci Eng, C 33:4994–5000

[41] Waldron K, Wu WD, Wu ZX, Liu WJ, Selomulya C, Zhao DY, Chen XD (2014) Formation of monodisperse mesoporous silica microparticles via spray-drying. J Colloid Interface Sci 418:225–233

[42] Cheow WS, Li S, Hadinoto K (2010) Spray drying formulation of hollow spherical aggregates of silica nanoparticles by experimental design. Chem Eng Res Des 88:673–685

[43] Lee SY, Gradon L, Janeczko S, Iskandar F, Okuyama K (2010) Formation of highly ordered nanostructures by drying micrometer colloidal droplets. ACS Nano 4:4717–4724

[44] Okuyama K, Abdullah M, Lenggoro IW, Iskandar F (2006) Preparation of functional nanostructured particles by spray drying. Adv Powder Technol 17:587–611

[45] Lv BY, Zhao LS, Pu Y, Le Y, Zeng XF, Chen JF, Wen N, Wang JX (2017) Facile preparation of controllable-aspect-ratio hydroxyapatite nanorods with high-gravity technology for bone tissue engineering. Ind Eng Chem Res 56:2976–2983

[46] Cao JM, Feng J, Deng SG, Chang X, Wang J, Liu JS, Lu P, Lu HX, Zheng MB, Zhang F, Tao J (2005) Microwave-assisted solid-state synthesis of hydroxyapatite nanorods at room temperature. J Mater Sci 40:6311–6313. https://doi.org/10.1007/s10853-005-4221-8

[47] Sideridou ID, Karabela MM (2009) Effect of the amount of 3-methacyloxypropyltrimethoxysilane coupling agent on physical properties of dental resin nanocomposites. Dent Mater 25:1315–1324

[48] Curtis AR, Palin WM, Fleming GJP, Shortall ACC, Marquis PM (2009) The mechanical properties of nanofilled resin-based composites: the impact of dry and wet cyclic pre-loading on bi-axial flexure strength. Dent Mater 25:188–197

[49] Halvorsona RH, Ericksona RL, Davidsonb CL (2003) The effect of filler and silane content on conversion of resin-based composite. Dent Mater 19:327–333

[50] Sadat-Shojai M, Atai M, Nodehi A, Khanlar LN (2010) Hydroxyapatite nanorods as novel fillers for improving the properties of dental adhesives: synthesis and application. Dent Mater 26:471–482

[51] Salehi S, Gwinner F, Mitchell JC, Pfeifer C, Ferracane JL (2015) Cytotoxicity of resin composites containing bioactive glass fillers. Dent Mater 31:195–203

[52] Goncalves F, Azevedo CL, Ferracane JL, Braga RR (2011) BisGMA/TEGDMA ratio and filler content effects on shrinkage stress. Dent Mater 27:520–526

[53] Wang ZZ, Landis FA, Giuseppettic AAM, Gibsona SL, Chianga MYM (2014) Simultaneous measurement of polymerization stress and curing kinetics for photo-polymerized composites with high filler contents. Dent Mater 30:1316–1324

[54] Lööfa J, Svahn F, Jarmar T, Engqvist H, Pameijer CH (2008) A comparative study of the bioactivity of three materials for dental applications. Dent Mater 24:653–659

[55] Yan SF, Yin JB, Cui L, Yang Y, Chen XS (2011) Apatite-forming ability of bioactive poly(L-lactic acid)/grafted silica nanocomposites in simulated body fluid. Colloids Surf B 86:218–224